

Implementation, Integration, and Verification of MIMAX WLAN Modem

Z. Stamenkovic

IHP

Frankfurt (Oder), Germany

stamenkovic@ihp-microelectronics.com

K. Tittelbach-Helmrich

IHP

Frankfurt (Oder), Germany

tittelbach@ihp-microelectronics.com

M. Wickert

Dresden University of Technology

Dresden, Germany

michael.wickert@tu-dresden.de

J. Ibanez

University of Cantabria

Santander, Spain

jesus@gtas.dicom.unican.es

S. Ruiz

TTI

Santander, Spain

sruiz@ttinorte.es

G. Dimosthenous

PrimeTel

Limassol, Cyprus

georgiosd@prime-tel.com

Abstract—This paper describes the concept, implementation, integration, and verification of an RF-MIMO wireless LAN system called MIMAX. A test setup for trying out the complete MIMAX modem in laptop form factor is presented. The purpose is to verify, debug, and improve all the components and entire system taking into account real-time operation parameters (traffic load, timing, error recovery, etc.). The correctness of the front-end specific MIMAX control functions like beamforming weights handling and setting has been verified. The compatibility with the standard SISO IEEE802.11a WLAN has also been proved.

Keywords-Baseband; MAC; MIMO; WLAN

I. INTRODUCTION

We have introduced a concept for multiple-input, multiple-output (MIMO) communication with signal weighting and combining near the transmitting and receiving antennas in the analogue front-end [1]-[4]. As a result of this paradigm shift, the customized integrated circuits and systems [5]-[8] have been developed that comply with the new requirements in relation to the front-end processing concept. Our RF-MIMO approach called MIMAX (MIMO for MAXimum reliability and performance) is compatible with the existing WLAN standard IEEE802.11a and able to achieve faster and more energy efficient data transmission. A system demonstrator has been developed to test and validate the MIMAX concept in real scenarios.

The paper gives a brief overview of the MIMAX system architecture and components. Then the implementation of the individual subsystems such as reconfigurable (in respect of the antenna number and channel conditions) medium access control (MAC) and baseband processors, analogue front-end circuits, and an antenna array is described. Finally, the system integration and verification aspects are presented.

II. SYSTEM ARCHITECTURE AND COMPONENTS

MIMAX operates compatibly to IEEE802.11a and amends the basic parts of this standard such as the physical and data link layer. Figure 1 shows the different communication layers investigated and developed in MIMAX. The MIMAX physical medium dependent layer consists of a new analogue front-end which performs the weighting and combining of multiple transmit and receive signals (in the conventional MIMO system, the digital baseband does it). It is controlled by an IEEE802.11a digital baseband which is extended for MIMAX specific operations. Likewise, the medium access control ensures data and control flow between the new baseband and the logical link control (LLC) layer. Finally, the compatibility to IEEE802 is achieved by a compliant LLC layer.

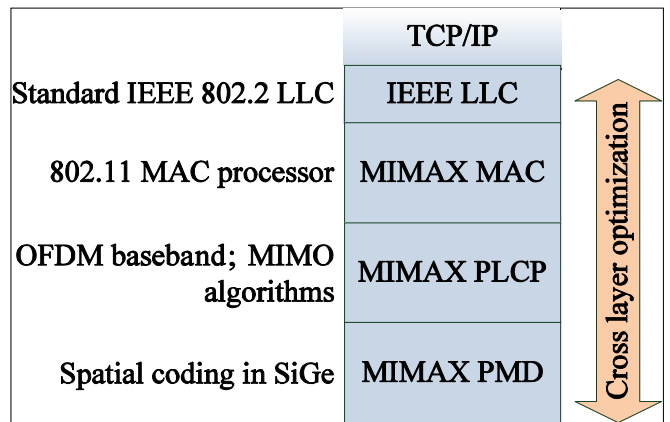


Figure 1. Communication layers addressed in MIMAX

The different functionalities of Figure 1 are integrated into separated subsystems that are assembled into a system demonstrator for verification and testing. These subsystems comprise a MAC processor, a baseband processor with RF

control unit (RFCU), an analogue transceiver, and an antenna array. As mentioned before, current wireless MIMO systems perform the processing and combining of the complex antenna signals in the digital baseband. Since the complete transmitter and receiver are required for each path, the resulting power consumption and costs of the conventional MIMO approaches [9] limit applications for ubiquitous networks. A low-power and low-cost RF-MIMO system significantly decreases the hardware complexity by performing the adaptive weighting and combining of the antenna signals in the RF front-end [10]-[12].

A. Analogue Front-End

A functional block diagram of the analogue front-end is shown in Figure 2. The transmitter uses a direct-up-conversion architecture. The baseband provides digital inphase and quadrature symbols that are converted in analogue signals using digital-to-analogue converters. These signals are up-converted to the carrier frequency and fed to all available antennas (the multiplexing gain equals one). Before transmitted to the air by the antenna, each signal is multiplied by a complex weight meaning adjusted in amplitude and phase relatively to the other paths. This multiplication is performed by a vector modulator [5]. Afterwards, the power amplifier drives the antenna.

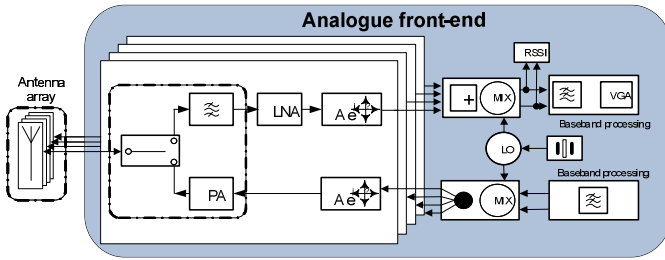


Figure 2. Analogue front-end architecture

The receiver is based on a direct down-conversion principle. The antenna unit is constructed of a four element array. In each receive path, a band pass filter is integrated to attenuate adjacent radio standards and to pass the 5GHz-band signals. The low noise amplifier (LNA) is integrated together with the vector modulator into a single subsystem and can be switched between high and low gain operation modes. The vector modulator performs the complex weight multiplication of the received signals, or equivalently changes the relative amplitudes and phases of all the antenna signals. Each of these received and weighted signals is then combined coherently and afterwards down-converted in the baseband to zero-IF. Consequently, the inphase and quadrature components are generated by a local oscillator and the combined signals are mixed with sinusoidal and cosinusoidal signals. These baseband signals are low pass filtered and then digitized by an analogue-to-digital converter for further processing by the digital baseband and the new MIMAX algorithms.

B. Digital Baseband

The digital baseband has to perform all tasks typical for the IEEE802.11a communication scheme and, additionally, MIMAX specific tasks like the MIMO channel estimation,

exploitation of the spatial diversity, and compensation of possible impairments in the RF spatial processing. The MIMO channel matrix has to be determined to allow the algorithms selecting the optimum weights [7]. For this purpose, a MIMAX transmitting device sends a training frame with several OFDM training symbols, but using for each OFDM symbol a different combination of orthogonal weights at the transmitting and the receiving device. The second MIMAX terminal receives these OFDM symbols, estimates the frequency-selective MIMO channel and computes the optimum weights based on the new algorithms. Then the former receiving device transmits a training frame and the initial transmitting device receives these OFDM symbols through its orthogonal weights and, then, estimates the frequency-selective MIMO channel and computes the optimum weights. The simplified architecture of the digital baseband is shown in Figure 3.

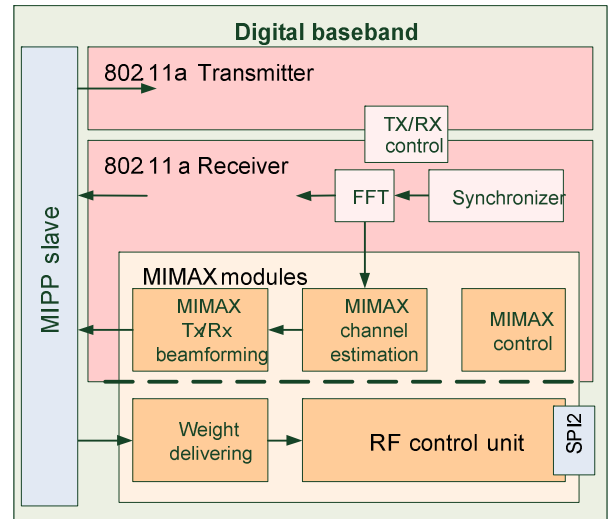


Figure 3. Digital baseband architecture

Integrating signal processing in the analogue circuits is limited by the maximum achievable resolution because of noise, process variations, and nonlinear behaviour of the devices. Therefore, the signal processing has to be calibrated by the digital baseband to adapt to the RF impairments. This mainly considers the correlation between real and imaginary parts of the vector modulator signals. Calibration is performed by the RF control unit in Figure 3. The characteristics of the vector modulator are analyzed by this module and stored in an internal memory. The weights provided by the baseband are then transferred into corresponding values of the vector modulator signal using the previously determined relationship and these new weights control now the vector modulator. Additional calibration options in the RF front-end and RF control unit allow an internal adaptation to impairments of the fabrication process and a feedback to the baseband processing. These techniques are based on look-up tables. The vector modulator is connected to the RF control unit by a serial peripheral interface (SPI).

C. MAC Layer

For the MIMAX data link control (DLC) layer, the standard IEEE802.2 logical link control layer is used on top of the

IEEE802.11 medium access control layer. The new functionalities of the MIMAX baseband processor impose some changes on the MAC protocol. It is necessary to know the configuration of the transceiver including the number of antennas at transmitter and receiver side and to maintain a database of active and available users (MAC addresses, last optimum weights, etc.). These tasks and the storage are related to MAC because no memory (except for the weight table in RF control unit) is available at the baseband processor. The MAC protocol has to control the data flow and specific instructions to the digital baseband depending on the communication scheme. It also initiates the MIMAX channel estimation procedure, which normally consists of a pair of training frames, exchanged between two stations. Another important MIMAX feature is the transmission of an RTS frame before each regular 802.11 frame. This is to allow the receiver to identify the transmitter of the frame and to set its receiver antenna configuration to the optimum weights for that connection before receiving the regular frame. There is a single RTS frame before each multicast or broadcast frame, and a RTC/CTS pair before each unicast frame. The MAC layer has been developed using the state machine approach and the specification and description language (SDL). Functionally complex or rarely used parts of the MAC protocol have been implemented in software. Time critical or software inefficient functions are swapped to dedicated hardware [13].

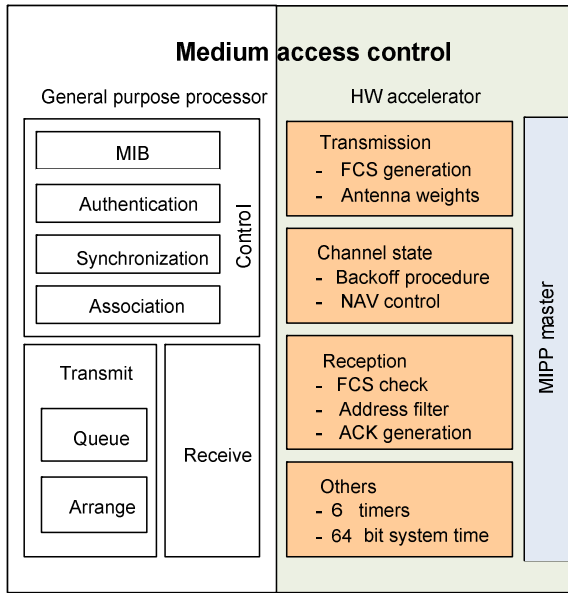


Figure 4. Hardware/software partitioning of the MAC layer

The hardware/software partitioning of the MAC layer is shown in Figure 4. A general purpose processor executes the software part and a hardware accelerator takes over buffering for the next frame, a cyclic redundancy check (CRC) and an optional encryption (in transmit direction), and CRC, frame address filtering, generation of acknowledgements and CTS frames and an optional decryption (in receive direction). Furthermore, a back-off procedure for frame sending, 6 timers, a system timer and several interfaces are provided as hardware modules. The interfaces include a 16-bit MIMAX EPP interface to the physical layer (MIPP), a CardBus interface to

the host computer, a serial RS232 interface for UART, and general purpose inputs/outputs.

III. IMPLEMENTATION

The developed algorithms, components, and subsystems have been implemented in hardware (except the MAC processor, which is a hardware/software co-design). The MIMAX modem prototype assembles the following hardware:

- An antenna array made up of 4 multiband microstrip planar F-shaped monopoles
- An analogue front-end that uses vector modulators as an analogue weighting circuitry
- An OFDM baseband processor that supports the new analogue front-end
- An enhanced MAC processor for MIMAX specific tasks and compatibility to 802.11a

A. Antenna Array

The MIMAX antenna array consists of four multiband radiating elements [14], [15] that provide dual band performance (2.4 GHz and 5 GHz bands operations). The considered form factor is determined by the laptop cover of 14.1" in size. The multiband antenna (Figure 5) is based on a microstrip-fed planar F-shaped monopole, printed on a FR4 substrate of thickness $h=0.5$ mm. The overall size of the antenna is 35.9 mm x 11.17 mm.

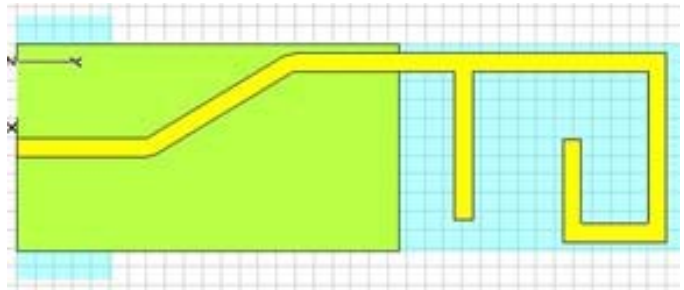


Figure 5. Multiband antenna

Two slots have been cut in the upper part of the antenna to obtain the desired resonance electric lengths without exceeding in size. In particular, the lower branch of the F-shaped antenna controls the resonance at 5.6 GHz, while the upper part determines the antenna resonance at 2.4 GHz. Both branches are designed to generate a resonant path for currents, which results to be less than a quarter of the free-space wavelength. It is important to observe that there is the need to obtain two $\lambda/4$ resonant paths at the two operating frequencies without exceeding in the size. Therefore, a curl path was designed in the upper part of the antenna, as shown in Figure 5.

This solution provides a control of the resonance at the lower frequency. Consequently, this antenna can be used for multi-standards such as 802.11a/b/g/n. The MIMAX antenna array has been designed using four multiband radiating elements. In order to keep low correlation between antennas, each radiator is placed in orthogonal position between them. In this way, polarization diversity is achieved.

B. Multi-IC Analogue Front-End

The multi-IC analogue front-end supports the transmitted and received signal weighting in RF domain. It consists of four low noise amplifiers and vector modulators, a signal combiner and the commercial MAX2828 RF integrated circuit chip for up/down-conversion. The printed-circuit-board with mentioned RF components is shown in Figure 6.

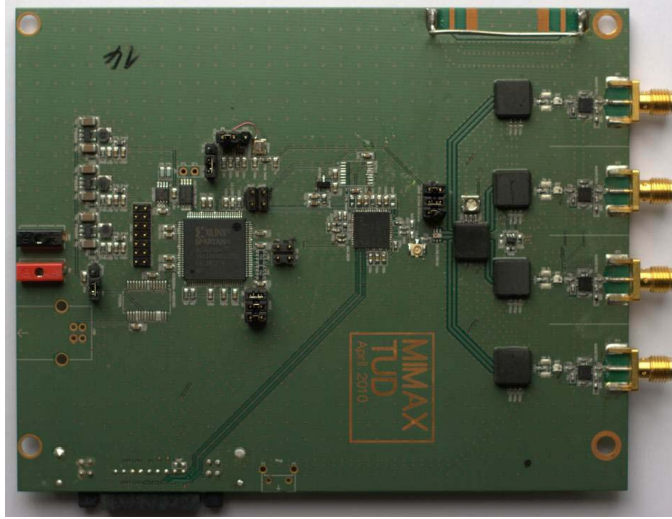


Figure 6. Multi-IC transceiver board

After successful assembly and fabrication of the multi-IC front-end, all the implemented functions have been tested and verified. The maximum available transmission power of +18 dBm has been measured. The weighting and combining has been verified by means of stepping through the available vector space. The calculated calibration tables can be used for compensation of any non-linear behaviour of the designed ICs.

C. Baseband Processor

The implementation of the baseband processor is based on two main blocks: the block that implements the parts compatible to the IEEE standard 802.11a and the block that assembles the modules for MIMAX channel estimation and beamformer selection (Figure 3). The conventional 802.11a processor includes the standard functionalities: mapping, channel encoding, pilot insertion, guard interval insertion, FFT/IFFT, Viterbi decoding, etc. The new functionalities are grouped into five main modules: channel estimation, beamforming, weight delivering, MIMAX control and RF control unit. Most of these MIMAX modules are active only when a MIMAX communication is detected by the Tx/Rx control block.

The MIMAX channel estimation block (Figure 3) estimates the $n_T \times n_R$ MIMO channel based on the $n_T \times n_R$ OFDM training symbols of the received training frame, where n_T and n_R stands for the number of antennas at transmitter and receiver side, respectively. It works in the frequency domain taking the FFT signal provided by the 802.11a processor as inputs and uses a least squares method. The MIMAX Tx/Rx beamforming uses the estimated MIMO channel as input, computes the optimal Tx/Rx weights, and transfers them to MAC. The channel estimation and beamforming blocks are started only when a

training frame is received, keeping the MIMAX baseband processor power consumption very close to the one of the conventional IEEE802.11a processor. Both blocks are reconfigurable in respect to the antenna number. They take into account the number of transmitter and receiver antennas (up to a maximum of 4) after extracting this information from the signal field of received training frame. The weight delivering module applies (from the baseband processor) the predefined set of weights during training and transferring the optimal or default weights during data transmission or reception. The MIMAX control module controls the signal and data flow among all MIMAX modules. It receives from the Tx/Rx control module the information included in the training frame signal field (number of Tx/Rx antennas, number of training symbols), as well as some activation and synchronization signals. Finally, RFCU controls the specific MIMAX functionalities of the analogue front-end through an SPI and compensates the impairments of the vector modulators.

D. MAC Processor

The MAC processor is based on two major digital chips located on a printed-circuit board in CardBus form factor:

- The general purpose processor (Figure 4) is an ASIC fabricated in the IHP's 0.25 μ m CMOS technology. It provides a MIPS 4KEp 32-bit microprocessor core and a CardBus (PCMCIA) interface to the host computer.
- A Xilinx Virtex-5 LX50 FPGA implements the MAC hardware accelerator and the MIPP interface (Figure 4).

The board contains many other components such as 4 MByte of processor flash memory and 1 MByte of RAM, clock generator, power supply for FPGA, configuration flash for FPGA, debugging and programming interfaces (RS232 interface for MAC firmware download and logic analyzer interface), status LEDs, etc.

The MIMAX MAC protocol is fully compatible with the IEEE standard 802.11. All the specific MIMAX features such as training frames and request-to-send (RTS) frames being transmitted before multicast frames are compatible with the standard and do not disturb normal traffic.

IV. INTEGRATION AND VERIFICATION

The implemented MIMAX components and subsystems have been integrated in a system prototype. The interactions between the subsystems and the system itself have been verified by simulations, measurement, and field tests.

First, the performance of the analogue front-end has been evaluated in standalone operation. This allows measuring major performance characteristics without the influence of other subsystems. Second, a setup composed of the antenna array, the multi-IC analogue front-end board, the baseband board and the MAC emulator has been tested. Using this setup, the authors have evaluated the critical operations involving the baseband and the analogue front-end, namely the weight setting during training and the weight uploading during data transmission. The correct operation of the vector modulators and combiner has been verified. Moreover, several indoor and

outdoor experiments to evaluate the physical layer performance of the MIMAX with respect to single-antenna terminals have been conducted.

On the other hand, a setup assembling the baseband processor, the MAC processor and the WLAN driver software has been used to debug and verify the interactions between mentioned subsystems under realistic conditions. Finally, the stability and robustness of the final MIMAX WLAN modem prototype has been demonstrated.

A. Standalone Verification of Analogue Front-End

A control FPGA and USB interface on the analogue front-end board allows the standalone verification of the design. Using a control program stored in FPGA, the major performance characteristics have been measured without the influence of other subsystems (baseband and MAC).

RF receiver characteristics have been observed for the signal path from the antenna input connector (SMA) to the input of the commercial RFIC including an adapter cable which is required for accessing the RF signal at this point. The measured characteristics are shown in Table 1.

TABLE I. RF RECEIVER CHARACTERISTICS

PARAMETER	VALUE
Gain	15.5 dB
Noise figure	7.4 dB
Input referred 1 dB compression	-34 dBm
Input referred 3rd order intersect point	-23.8 dBm
Power consumption	180 mW

The excellent weighting capabilities of the receiver vector modulator chips and the subsequent signal combiner chip are shown in Figure 7.

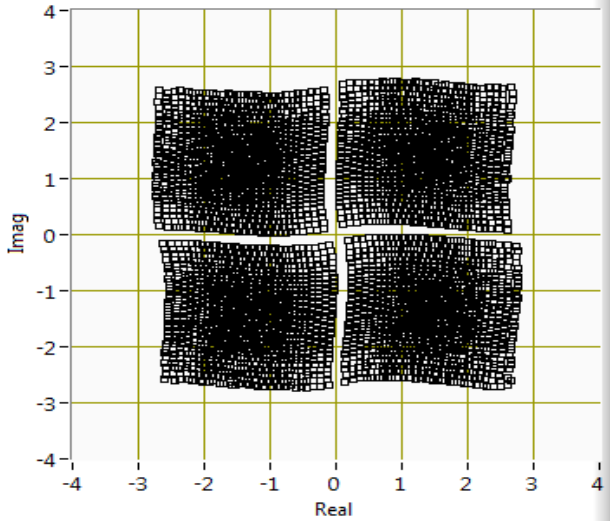


Figure 7. Weighting behaviour of the vector modulators

RF transmitter characteristics for the signal path from the output of the MAX2828 to the antenna connector (the power amplifier, antenna selector switch and Rx/Tx switch) are shown in Table 2. Again, an adapter cable is incorporated for feeding signals to the power amplifier input.

TABLE II. RF TRANSMITTER CHARACTERISTICS

PARAMETER	VALUE
Gain	26 dB
Input reflection	<-10 dB
Max. antenna branch leakage	-8 dB

B. Analogue Front-End and Digital Baseband

The setup depicted in Figure 8 has been used to verify the correct operation of the vector modulators under the baseband processor control. Moreover, extensive indoor and outdoor experiments have been conducted in order to perform a low level characterisation of the MIMAX system, using as figures of merit the frame error rate (FER), the RSSI level after combining (power of the received signal after combining), and the SNR gain. These values can easily be translated into coverage improvement or increased rate in comparison to SISO system.

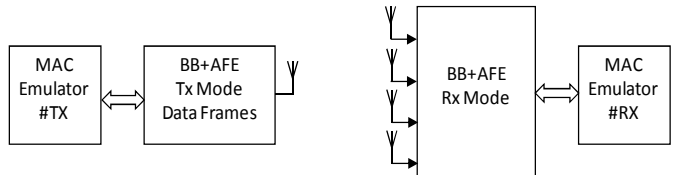


Figure 8. Test setup for verification of the physical layer

The experiments were performed using one transmitting antenna, four receiving antennas, central frequency of 5.26 GHz, and several frame formats (10 or 20 OFDM symbols length and 9, 18, 36, or 54 Mbps). Several distances between transmitter and receiver have been considered ranging from 8 to 20 meters in NLOS indoor scenarios and from 15 to 50 meters in LOS outdoor scenarios.

The procedure consisted of a SISO evaluation stage in which 100 data frames are transmitted and received using default weights, which means that the same weights were applied to the 4 receiving antennas, showing the behaviour of an equivalent SISO system. In the MIMAX evaluation stage a training frame is transmitted and the receiving baseband processor computed the optimal weights. Then, the optimal weights are applied and 100 data frames are received. This procedure was repeated 25 times at each location and for each frame format by moving the receiver within a small local area (i.e. 900 cm²).

As an example, Table 3 shows the comparison between SISO and MIMAX when transmitter and receiver were placed 12 meters apart in an indoor scenario. For instance, the MIMAX FER at 36 Mbps is 2.3%, whereas a SISO system (using default weights in the MIMAX prototype) the FER increases to 41.8%. Using 64-QAM, the MIMAX FER is close to 24%, and for SISO it goes up to 86%. From a practical point of view, this means that in SISO we are limited to 18 Mbps, while MIMAX allow us to double the rate and transmit at 36 Mbps with similar FER or we can even work at 54 Mbps. In terms of power, the gain of MIMAX versus SISO is 7 dB: this roughly means that with MIMAX we could have increased the coverage by a factor of two. Similar results were obtained for the rest of indoor and outdoor scenarios, showing the benefits of using MIMAX in comparison with SISO.

TABLE III. PHY LAYER BENCHMARKING

		FER (%)	RSSI (dBm)	Power Gain (dB)
BPSK 9Mbps	SISO	1.3	-58.7	7
	MIMAX	0.0	-52.3	
	SISO	11.0	-59.0	
	MIMAX	0.1	-51.3	
	SISO	41.8	-58.5	
	MIMAX	2.3	-51.4	
	SISO	85.8	-59.1	
64QAM 54Mbps	MIMAX	23.9	-52.2	

C. Digital Baseband and MAC

A test setup that connects two MIMAX stations with a cable in place of the analogue front-ends has been used to verify the operation and performance of MAC and digital baseband. Each station consists of the following subsystems: a laptop computer running Linux and the WLAN driver software, the MAC board plugged in to the CardBus slot of the laptop and the baseband board connected to MAC via the MIPP cable (Figure 9). This way a system assembling the real MAC layer and digital baseband has been tested in the conditions of an ideal radio channel. MIMO effects cannot be investigated with this setup.



Figure 9. Photo of a system assembling the MAC and baseband boards

The monitor right in the background of Figure 9 shows the constellation diagram. The video is transferred from the laptop in the back using the 16-QAM signal modulation. The laptop screen in the left displays the received video. One can also recognise the windows of the MIMAX traffic monitor programme (with the yellow and orange bars, which visualise the optimal weight settings) and the terminal programme which controls connection setup and other WLAN parameters.

The primary goal of this test setup is to improve the stability and robustness of the MAC and baseband processors, as well as the WLAN driver software in real-time conditions. Moreover, the signal quality (constellation diagram) and data throughput can be measured for the ideal radio link. The MAC data throughput has been estimated by measuring the time required to copy a large file. The measurement is done at the

Linux driver. Thus, it includes the MAC protocol overhead due to frame preambles, acknowledgements and RTS/CTS, the WLAN driver overhead, and other limiting effects like MAC firmware performance limitations. Therefore the measured throughput is expected to be smaller than the nominal physical layer data rate. The measurement results in Mbit/s and in % of the nominal PHY data rate are shown in Table 4. Since the overhead (e.g. frame preambles, duration of an ACK frame) does not scale as the physical data rate increases, the relative throughput degrades very fast with increasing the data rate, which is normal in WLAN [16].

TABLE IV. DATA THROUGHPUT OF DRIVER, MAC AND BASEBAND

MODULATION	BPSK	QPSK	16-QAM	64-QAM
Nominal data rate	6	12	24	48
Throughput without RTS/CTS	4.4 73%	7.2 60%	10.6 44%	13.0 27%
Throughput with RTS/CTS	4.1 68%	6.6 55%	9.2 38%	11.5 24%

The longer the frame is, the smaller is the overhead, and, consequently, the higher is the performance. Table 4 also compares the throughputs of the standard IEEE 802.11 mode and the MIMAX mode with RTS and CTS. These short frames impose an additional overhead. However, at least in a multiuser MIMAX scenario, they are required for the receiver to identify the transmitting station and to set the optimal weights for that link before receiving a long frame. The loss can be overcompensated by the higher physical data rate selected when setting the optimal weights. The simulation results for this behaviour are shown in Figure 10. The black curve shows the normal 802.11 throughput at a physical data rate of 6 Mbit/s as a function of the packet size. The red curve is the MIMAX throughput with RTS and CTS. Due to the additional overhead, this throughput is lower than the normal. However, since the MIMAX technology improves the link quality, allowing for higher physical data rates, the loss due to RTS/CTS overhead is overcompensated for frame sizes above 100 bytes (at 6 Mbit/s). The loss can be further minimised by transmitting several data frames within the RTS/CTS interval.

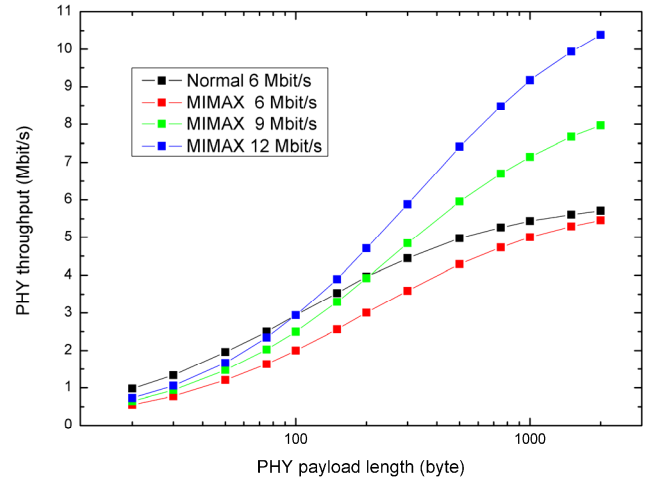


Figure 10. Physical layer data throughput as a function of the packet size

The measured data in Table 4 are little worse than the curves in Figure 10 since the simulations are done for the

physical layer only. They take into account the data frame itself, acknowledgement, RTS/CTS frames and relevant SIFS times. The additional overhead sources like backoff periods, MAC header length, beacons, etc. are not included.

D. Verification of Complete System

A setup for trying out the complete MIMAX system (antenna array, analogue front-end board, baseband board, MAC board and WLAN driver) has finally been assembled. The purpose is to debug, improve and verify the system in real-time conditions and to prove its better performance (as well as, the compatibility) in comparison with the standard 802.11a WLAN.

The baseband and analogue front-end boards have been mounted into the housing which was developed to make the MIMAX demonstrator laptop-compact and small. A photo of the system test setup is shown in Figure 11. The monitor displays a good example of the QPSK constellation diagram. Next to the antenna, the front-end and baseband boards mounted into the black MIMAX housing are visible. In the foreground right is the MAC board. Right on the screen, the MIMAX traffic monitor can be seen. The lower bar with many blue stripes shows the transmitted frames and the upper bar with short green stripes shows the received frames. Single red lines in between indicate the training frames. The orange and yellow bars on top visualise the weight settings (I and Q components) for three antennas.



Figure 11. Photo of the complete system test setup

This setup has been used in two configurations: one made of two MIMAX stations to evaluate a pure MIMAX WLAN with the MIMAX specific features (in particular, handling of training frames), and the other made of a MIMAX station and a commercial 5 GHz WLAN access point to verify the MIMAX compatibility with the standard 802.11a WLAN. In second configuration, the MIMAX features (RTS/CTS and training frames) are disabled since the access point cannot correctly handle them.

Test scenarios are similar to those described in the previous section. Some frame transfer statistics on Linux WLAN driver level is shown in Figure 12. In case of a MIMAX station and a

commercial access point, a file of about 40 Mbyte has been copied from a computer somewhere in the fixed network via the access point to the MIMAX station. The BPSK modulation scheme has been used since the access point was set to transmit at 6 Mbit/s. The higher network layers (TCP/IP) try to achieve the optimum data throughput under given transfer conditions. The WLAN driver monitors frame transfer statistics including retransmissions.

```
Frame statistics: 69.17 s elapsed since last call
24786 frames with 34.8 Mbytes received, rate 515 kbyte/s
12925 frames with 715 kbytes transmitted, rate 10.3 kbyte/s
2 TxFailed = 0% 1453 TxRetried = 11% 2199 retries in total
992 Rtry[1] = 7% 279 Rtry[2] = 2% 182 Rtry[more]
```

Figure 12. Frame transfer statistics for a file transfer using BPSK modulation

The mean data rate is $515 \text{ kbyte/s} = 4.12 \text{ Mbit/s}$ in receive direction and $10 \text{ kbyte/s} = 0.08 \text{ Mbit/s}$ in transmit direction (TCP-level acknowledgements). It is 4.2 Mbit/s in total. The rest up to the nominal data rate of 6 Mbit/s is due to the MAC overhead (MAC level acknowledgements, beacons, backoff periods and preambles), the data frame overhead (MAC header, SNAP header, etc.), the traffic related to other stations in LAN and collisions/retransmissions due to bad channel conditions. For two frames out of 12925, the transmission finally failed after seven retries; 992 frames were retransmitted once; 279 frames twice; and 182 frames more often. The CRC error frequency in received frames is not reported but is normally of the same order.

V. CONCLUSION

MIMAX technology integrates the concept for short range communication, in particular for an IEEE802.11a wireless local area network, introducing MIMO communication modes but still offering compatibility to legacy devices. The project has developed a system prototype for a proof-of-concept, testing and performance evaluation. The prototype contains the customised hardware and software systems which enable MIMO modes and ensure compatibility.

System architecture, design, implementation, integration and verification are presented. The MIMAX technology is evaluated with respect to the competing wireless radio technologies such as SISO systems. The improvement in performance is shown in terms of technical parameters (frame error rates) and user show-cases (transmission of video streams).

ACKNOWLEDGMENT

The research leading to these results has received funding from the European Community's Seventh Framework Programme FP7 (2007 - 2013) under the grant agreement no. 213952 also referred as MIMAX.

REFERENCES

- [1] I. Santamaría, V. Elvira, J. Via, D. Ramirez, J. Perez, J. Ibanez, R. Eickhoff, and F. Ellinger, "Optimal MIMO transmission schemes with adaptive antenna combining in the RF path," *Proc. 16th European Signal Processing Conference*, Lausanne (Switzerland) 2008, (pp. 1-5)

- [2] R. Eickhoff, R. Kraemer, I. Santamaria, and L. Gonzalez, "Developing energy-efficient MIMO radios," *IEEE Vehicular Technology Magazine*, vol. 4, pp. 34-41, 2009.
- [3] J. Via, V. Elvira, I. Santamaria and R. Eickhoff, "Analog antenna combining for maximum capacity under OFDM transmissions," *Proc. IEEE Inter. Conference on Communications*, Dresden (Germany) 2009, (pp. 1-5)
- [4] Z. Stamenkovic, K. Tittelbach-Helmrich, M. Krstic, J. Perez, J. Via, and J. Ibanez, "Architecture of an analog combining MIMO system compliant to IEEE802.11a," *Proc. ICT-MobileSummit 2009*, Santander (Spain) 2009, (pp.1-8)
- [5] N. Joram, U. Mayer, R. Eickhoff, and F. Ellinger, "Fully integrated active CMOS vector modulator for 802.11a compliant diversity transceivers," *Proc. International IEEE Conference on Microwaves, Communications, Antennas and Electronic System*, Tel-Aviv (Israel) 2009, (pp. 1-4)
- [6] J. Via, V. Elvira, I. Santamaria, and R. Eickhoff, "Minimum BER beamforming in the RF domain for OFDM transmissions and linear receivers," *Proc. IEEE International Conference on Acoustics, Speech and Signal Processing*, Taipei (Taiwan) 2009, (pp. 2513-2516)
- [7] V. Elvira, J. Ibanez, I. Santamaria, M. Krstic, K. Tittelbach-Helmrich, and Z. Stamenkovic, "Baseband processor for RF-MIMO WLAN," *Proc. 17th IEEE International Conference on Electronics, Circuits, and Systems*, Athens (Greece) 2010, (pp. 798-801)
- [8] K. Tittelbach-Helmrich, E. Miletic, P. Wcislek, and Z. Stamenkovic, "MAC hardware platform for RF-MIMO WLAN," *Proc. 53rd IEEE International Midwest Symposium on Circuits and Systems*, Seattle (USA) 2010, (pp. 339-342)
- [9] H. Boelcskei, D. Gesbert, C. B. Papadimas, and A.-J. van der Veen, *Space-Time Wireless Systems: From Array Processing to MIMO Communications*, Cambridge University Press, Cambridge 2006.
- [10] F. Ellinger and W. Baechtold, "Adaptive antenna receiver module for WLAN at C-band with low power consumption," *IEEE Microwave and Wireless Components Letters*, vol. 12, pp. 348-350, 2002.
- [11] J. Via, I. Santamaria, V. Elvira, and R. Eickhoff, "A general criterion for analog Tx-Rx beamforming under OFDM transmissions," *IEEE Trans. on Signal Processing*, vol. 58, pp. 2155-2167, 2010.
- [12] A. Jahanian, F. Tzeng, and P. Heydari, "Code modulated path sharing multi-antenna receivers: theory and design," *IEEE Trans. Wireless Communications*, vol. 8, pp. 2193-2201, 2009.
- [13] Z. Stamenkovic, E. Miletic, M. Obrknezev, and K. Tittelbach-Helmrich, "MAC protocol implementation in RF-MIMO WLAN," *Proc. 16th IEEE International Conference on Electronics, Circuits, and Systems*, Yasmine Hammamet (Tunisia) 2009, (pp. 303-306)
- [14] O. Gago, L. Gonzalez, and R. Eickhoff, "Study of the optimum number of radiating elements for different portable devices operating in a MIMO system," *Proc. the European Wireless Conference*, Aalborg (Denmark) 2009.
- [15] O. Gago, L. Gonzalez, R. Eickhoff, and I. Santamaria, "MIFA: Modified IFA radiating element for small handheld devices," *Proc. the 18th ICT MobileSummit*, Santander (Spain) 2009.
- [16] G. Bianchi, "Performance analysis of the IEEE 802.11 distributed coordination function," *IEEE Journal on Selected Areas in Communications*, vol. 18, pp. 535-547, 2000.